

Illumination Planning for Measuring Per-Pixel Surface Roughness

Kota Arieda Takahiro Okabe
Kyushu Institute of Technology
okabe@ai.kyutech.ac.jp

Abstract

Measuring per-pixel surface roughness is useful for machine vision applications such as visual inspection. The surface roughness can be recovered from specular reflection components, but a large number of images taken under different lighting and/or viewing directions is required in general so that sufficient specular reflection components are observed at each pixel. In this paper, we propose a robust and efficient method for per-pixel estimation of surface roughness. Specifically, we propose an illumination planning based on noise propagation analysis; it achieves the surface roughness estimation from a small number of images taken under the optimal set of light sources. Through the experiments using both synthetic and real images, we experimentally show the effectiveness of our proposed method and our setup with a programmable illumination and a polarization camera.

1 Introduction

The appearance of an object surface is described by the reflectance properties, *i.e.* BRDFs for opaque surfaces and BSSRDFs for translucent surfaces. The reflectance properties depends on surface materials such as metals, plastics, and silicons and their surface states such as rust, cracks, and scratches. Therefore, estimating the reflectance properties of object surfaces is useful not only for photorealistic image synthesis but also for visual inspection of object surfaces such as metallic surfaces [18, 11, 10, 9, 14] and printed circuit boards [12, 7]. In this study, we propose an image-based method for measuring the reflectance properties of object surfaces, in particular per-pixel surface roughness in a non-contact and non-destructive manner.

In general, specular reflection reflects the light incoming from a light source to a narrow range of directions, while diffuse reflection uniformly reflects the light, *e.g.* the radiance of a Lambertian surface is independent of viewpoints. For a smooth surface, specular reflection reflects the light to the mirror-reflection direction, *i.e.* the outgoing angle is the same as the incoming angle, and then we observe sharp specular highlights. As the roughness of an object surface increases, the specular reflection reflects the light to a broader range of directions, and then we observe more blurred specular highlights. Therefore, we can estimate

the surface roughness on the basis of specular reflection observed on an object surface.

In order to measure per-pixel surface roughness, we need to observe specular reflection components at each pixel under different lighting and/or viewing directions in general so that they are sufficiently observed at each pixel. Therefore, a large number of images is required for measuring per-pixel surface roughness; the number of required images increases as the surface roughness decreases, because the specular highlights are sharper for smoother surfaces. In addition, acquiring a large number of images with different light source and/or camera positions by mechanically moving a light source and/or a camera is time consuming.

Accordingly, in this paper, we propose a robust and efficient method for measuring per-pixel surface roughness. The key idea of our proposed method is illumination planning on the basis of noise propagation analysis. Specifically, our method estimates per-pixel surface roughness of the Torrance-Sparrow model [13] from the images taken under the optimal set of light sources by taking noises in pixel values into consideration. It is contrast to the existing technique [3] for robust and efficient photometric stereo; the estimation of surface normal assuming the Lambert model [16]. In addition, our setup makes use of an LCD as a programmable polarized illumination and a polarization camera for distinguishing a specular reflection component from diffuse and subsurface scattering components.

The main contribution of this paper is twofold. First of all, we propose an illumination planning for estimating per-pixel surface roughness. Specifically, we study the noise propagation in surface roughness estimation, and derive how to select the optimal light sources for robustly and efficiently estimating surface roughness from a small number of images. Second, we confirmed the effectiveness of our method through the experiments using our prototype setup. Our setup efficiently controls light source positions with an LCD and robustly extracts specular reflection components using a polarization camera.

2 Related Work

Our proposed method is related to the recovery of spatially-varying reflectance functions. Since the recovery of spatially-varying reflectance is often under-constrained, in particular when specular reflection does

not observed at a surface point, data-driven approaches has been studied.

Alldrin *et al.* [1], Hui and Sankaranarayanan [5], and Hui *et al.* [6] propose methods for estimating spatially-varying reflectance by using both the multiple images with photometric stereo setup and a collocated camera and light source, and the prior knowledge with respect to spatially-varying BRDFs such as basis BRDFs and their dictionary. Recently, deep learning based approach is studied [8, 17, 2, 4]. They achieve the recovery of spatially-varying reflectance even from a single image.

In contrast to the above methods, our proposed method is the direct measurement of surface roughness, and therefore need not collect the training data and achieves per-pixel recovery independent of other pixels. In addition, our formulation enables us to predict the accuracy (MSE) of the estimated parameters (see Section 3.2 for more details).

3 Proposed Method

Our proposed method assumes that the position of a camera, the positions of light sources, and the normal of a surface point are known in advance, and then estimates two parameters of the Torrance-Sparrow model, *i.e.* surface roughness and specular reflectance per pixel. In this Section, we show that the estimation of surface roughness results in weighted least squares and that the optimal light sources can be selected on the basis of noise propagation analysis. Then, we describe the illumination planning for robustly and efficiently estimating surface roughness.

3.1 Estimation of Surface Roughness

According to the (simplified) Torrance-Sparrow model [13], the pixel value of specular reflection component i observed at a surface point is represented by

$$i = \frac{k}{\mathbf{n}^\top \mathbf{v}} e^{-\frac{\beta^2}{2s^2}}, \quad (1)$$

where the specular reflectance k and the surface roughness s are unknowns to be estimated. We assume that the surface normal \mathbf{n} , the viewing direction \mathbf{v} , and the angle β between the surface normal and the half vector are known.

We assume that the observed pixel value is contaminated by additive noise δ as

$$i = \frac{k}{\mathbf{n}^\top \mathbf{v}} e^{-\frac{\beta^2}{2s^2}} + \delta. \quad (2)$$

We take logarithm of eq.(2), and then obtain

$$i \begin{pmatrix} 1 & \beta^2/2 \end{pmatrix} \begin{pmatrix} -\ln k \\ 1/s^2 \end{pmatrix} = -i \ln[(\mathbf{n}^\top \mathbf{v})i] + \delta, \quad (3)$$

since $\ln(i - \delta) \simeq (\ln i - \delta/i)$ when $\delta \ll i$.

Our proposed method estimates the specular reflectance and surface roughness from multiple images taken under different light sources. We denote the pixel value, the angle between the surface normal and the half vector, and the noise under the l -th light source ($l = 1, 2, 3, \dots, L$) by i_l , β_l , and δ_l respectively. Then, the set of linear equations, *i.e.* the constraints imposed by the observed pixel values are represented as

$$\mathbf{W}\mathbf{B} \begin{pmatrix} -\ln k \\ 1/s^2 \end{pmatrix} = -\mathbf{W}\mathbf{a} + \boldsymbol{\delta}. \quad (4)$$

Here, \mathbf{W} , \mathbf{B} , \mathbf{a} , and $\boldsymbol{\delta}$ are given by

$$\mathbf{W} = \begin{pmatrix} i_1 & & & 0 \\ & i_2 & & \\ & & \ddots & \\ 0 & & & i_L \end{pmatrix}, \quad \mathbf{B} = \begin{pmatrix} 1 & \beta_1^2/2 \\ 1 & \beta_2^2/2 \\ \vdots & \vdots \\ 1 & \beta_L^2/2 \end{pmatrix}, \quad (5)$$

$\mathbf{a} = (\ln[(\mathbf{n}^\top \mathbf{v})i_1], \ln[(\mathbf{n}^\top \mathbf{v})i_2], \dots, \ln[(\mathbf{n}^\top \mathbf{v})i_L])^\top$, and $\boldsymbol{\delta} = (\delta_1, \delta_2, \dots, \delta_L)^\top$.

Therefore, we set $\boldsymbol{\delta} = \mathbf{0}$ in eq.(4), and estimate the specular reflectance and surface roughness by solving the set of linear equations as

$$\begin{pmatrix} -\ln k \\ 1/s^2 \end{pmatrix} = -(\mathbf{W}\mathbf{B})^+ \mathbf{W}\mathbf{a}. \quad (6)$$

Here, $(\mathbf{W}\mathbf{B})^+$ is the pseudo inverse matrix of $(\mathbf{W}\mathbf{B})$, *i.e.* $(\mathbf{W}\mathbf{B})^+ = [(\mathbf{W}\mathbf{B})^\top (\mathbf{W}\mathbf{B})]^{-1} (\mathbf{W}\mathbf{B})^\top$. Intuitively, eq.(4) and eq.(5) say that the l -th light source is not useful when $i_l \simeq 0$ or $\exists l', \beta_l \simeq \beta_{l'}$.

3.2 Selection of Light Sources

Let us denote the estimated and ground truth parameters of the Torrance-Sparrow model, *i.e.* $(-\ln k, 1/s^2)^\top$ at a surface point by \mathbf{x} and $\bar{\mathbf{x}}$ respectively. We study the variance-covariance matrix $\boldsymbol{\Sigma}$ of the parameters defined by

$$\boldsymbol{\Sigma} = E[(\mathbf{x} - \bar{\mathbf{x}})(\mathbf{x} - \bar{\mathbf{x}})^\top], \quad (7)$$

where $E[\]$ stands for the expectation values.

Substituting eq.(4) into eq.(7), we can derive

$$\begin{aligned} \boldsymbol{\Sigma} &= E[(\mathbf{W}\mathbf{B})^+ \boldsymbol{\delta} \{(\mathbf{W}\mathbf{B})^+ \boldsymbol{\delta}\}^\top] \\ &= E[(\mathbf{W}\mathbf{B})^+ \boldsymbol{\delta} \boldsymbol{\delta}^\top \{(\mathbf{W}\mathbf{B})^+\}^\top] \\ &= \sigma^2 (\mathbf{W}\mathbf{B})^+ \{(\mathbf{W}\mathbf{B})^+\}^\top \\ &= \sigma^2 (\mathbf{B}^\top \mathbf{W}^2 \mathbf{B})^{-\top}, \end{aligned} \quad (8)$$

where we assume independent and identically distributed noises whose mean and variance are 0 and σ^2 respectively. Since the mean square error (MSE) is proportional to the trace of the variance-covariance matrix, we obtain the MSE of the parameters as

$$\text{MSE} \propto \text{Tr}[(\mathbf{B}^\top \mathbf{W}^2 \mathbf{B})^{-\top}]. \quad (9)$$

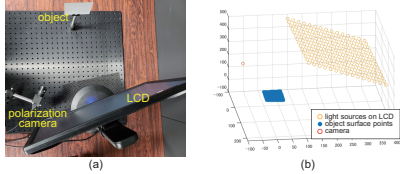


Figure 1. Experimental environment: (a) our setup and (b) its geometry.

Our proposed method iteratively selects the optimal light source for reducing the MSE (see Section 3.3 for more details). Since we have P pixels in total, our method selects the light source so that

$$\sum_{p=1}^P \text{Tr}[(\mathbf{B}_p^\top \mathbf{W}_p^2 \mathbf{B}_p)^{-1}] \quad (10)$$

is minimized. Here, \mathbf{B}_p and \mathbf{W}_p stand for the matrices in eq.(5) at the p -th pixel ($p = 1, 2, 3, \dots, P$).

3.3 Illumination Planning

We can see that the optimal set of light sources depend not only on the known geometry but also on the unknown parameters of the Torrance-Sparrow model through the matrix \mathbf{W}_p in eq.(10). Accordingly, we propose two approaches: online and offline illumination plannings.

The online illumination planning iteratively adds light sources for reducing the MSE of the estimated parameters, where the parameters for computing the pixel values in eq.(10) are updated every time the light source is added. Specifically, when we select the $(l+1)$ -th light source, we compute the pixel values under the $(l+1)$ -th light source by using the specular reflectance and surface roughness estimated from the l images.

The offline illumination planning assumes that some estimates of the parameters are known and then computes the optimal set of light sources in advance. As the surface roughness decreases, the specular highlights become sharper and the larger number of light sources distributed more densely is required. Therefore, the optimal set of light sources are computed from the lower limit of the surface roughness of an object of interest.

4 Experiments

4.1 Experimental Environment

To confirm the effectiveness of our proposed method, we conducted experiments using both synthetic and real images. In the experiments using real images, we used the setup consisting of an LCD and a polarization camera as shown in Figure 1 (a). Specifically, we displayed white blocks on the LCD and used them as polarized light sources; the total number of light sources

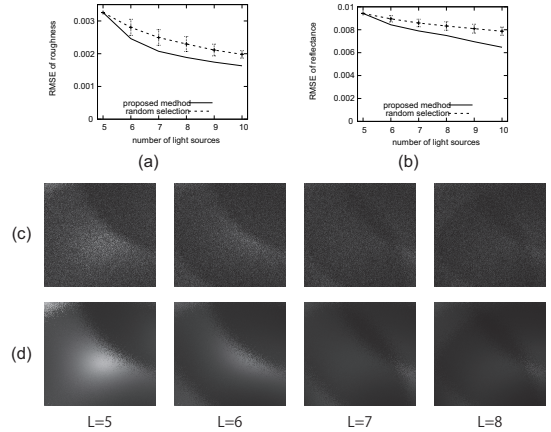


Figure 2. Experimental results using synthetic images: uniform surface.

is 210. The images of an object of interest were captured by using the polarization camera BFS-U3-51S5P-C from FLIR and the specular reflection components were extracted from those images [15]. We assumed planar objects as is often the case with CV-based visual inspection [18, 11, 12, 7, 10, 9, 14]. The geometry among the light sources, the points on the object surface, and the camera was calibrated by using MATLAB camera calibration toolbox in advance (see Figure 1 (b)). In the experiments using synthetic images, we rendered the images with the same geometry, and added zero-mean Gaussian noises to them whose standard deviation is 0.01 for the pixel values scaled from 0 to 1.

We compared our proposed online illumination planning with the random selection of light sources. Specifically, both the methods empirically select initial light sources from 210 light sources so that we can observe specular reflection components under at least two light sources at each pixel, because we have two unknowns to be estimated. Then, our method iteratively adds the image taken under the optimal light source that minimizes the sum of traces in eq.(10) and updates the surface roughness and specular reflectance. We find the optimal light source from the 210 candidates in a brute force manner. The random selection iteratively adds the image taken under a randomly selected light source and computes the surface roughness and specular reflectance. The number of trials for the random selection was 50.

4.2 Results Using Synthetic Images

First, we tested a surface with uniform reflectance properties; $s = 0.05$ and $k = 0.3$. Figure 2 shows (a) the RMSEs of the estimated surface roughness and (b) the RMSEs of the estimated specular reflectance vs. the number of light sources. The solid and dotted lines

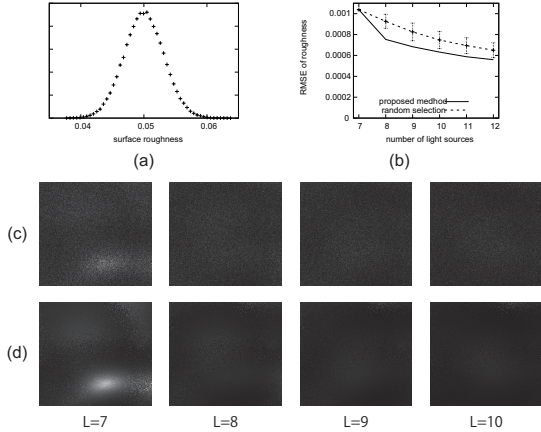


Figure 3. Experimental results using synthetic images: nonuniform surface.

stand for the RMSEs of our method and the random selection respectively. The error bars stand for the range of ± 1 sigma. We can see that the RMSEs of both our method and the random selection decrease as the number of light sources increases. In particular, we can see that the RMSE of our method is smaller than that of the random selection. In other words, our illumination planning achieves the same accuracy with a smaller number of light sources than the random selection.

Figure 2 visualizes (c) the error map of the surface roughness estimated by using our proposed method and (d) the trace map in eq.(10), when the number of light sources increases from 5 to 8. Here, the larger is the brighter. We can see that the traces are correlated with the errors of the estimated surface roughness, and the light sources are added so that they reduce the traces. This shows the effectiveness of selecting light sources on the basis of the sum of traces.

Second, we tested a surface with non-uniform reflectance properties; the distribution of surface roughness is shown in Figure 3 (a). Figure 3 (b) shows the RMSEs of the estimated surface roughness vs. the number of light sources. Similar to the above result for the uniform surface, we can see that the RMSE of our method is smaller than that of the random selection. We obtained the similar results to the above as to the error map of the estimated surface roughness and the trace map as shown in Figure 3 (c)(d). Those results support the effectiveness of our method for nonuniform surfaces.

4.3 Results Using Real Images

In the experiments using real images, we tested a ground glass with almost uniform reflectance properties. We considered the surface roughness estimated from all of the 210 images as the ground truth. Figure 4 (a) shows the distribution of the surface roughness.

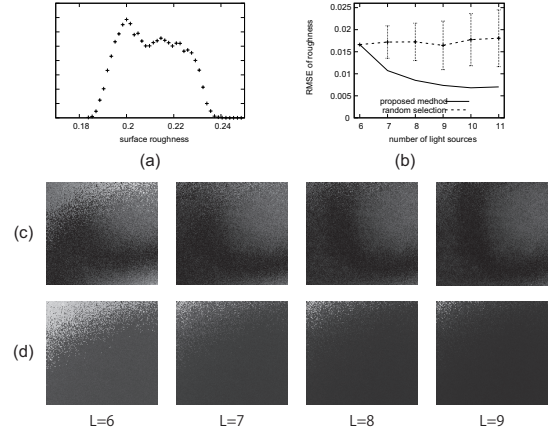


Figure 4. Experimental results using real images: ground glass.

Figure 4 (b) shows the RMSEs of the estimated surface roughness vs. the number of light sources. The solid and dotted lines stand for the RMSEs of our method and the random selection respectively. We can see that the RMSE of our method is smaller than that of the random selection.

Figure 4 visualizes (c) the error map of the surface roughness estimated by using our proposed method, and (d) the trace map in eq.(10), when the number of light sources increases from 6 to 9. We can see that the traces are correlated with the errors of the estimated surface roughness, and the light sources are added so that they reduce the traces. Those results show the effectiveness of our proposed method for real images.

5 Conclusion and Future Work

In this paper, we proposed a method for estimating per-pixel surface roughness on the basis of specular reflection components. Specifically, we studied the noise propagation in surface roughness estimation, and derived how to select the optimal light sources for robustly and efficiently estimating surface roughness from a small number of images. We confirmed the effectiveness of our method through the experiments using our prototype setup consisting of a programmable polarized illumination and a polarization camera.

Currently, our method assumes planar surfaces as is often the case with CV-based visual inspection. The extension to curved surfaces is one of the future direction of our method.

Acknowledgment

This work was supported by JSPS KAKENHI Grant Numbers JP20H00612 and JP17H01766.

References

- [1] N. Alldrin, T. Zickler, and D. Kriegman, “Photometric stereo with non-parametric and spatially-varying reflectance”, In Proc. IEEE CVPR2008, pp.1–8, 2008.
- [2] V. Deschaintre, M. Aittala, F. Durand, G. Drettakis, and A. Bousseau, “Single-image SVBRDF capture with a rendering-aware deep network”, ACM ToG, 37(4), pp.1–15, 2018.
- [3] O. Drbohlav and M. Chantler, “On optimal light configurations in photometric stereo”, In Proc. IEEE ICCV 2005, pp.II-1707–1712, 2005.
- [4] D. Gao, X. Li, Y. Dong, P. Peers, K. Xu, and X. Tong, “Deep inverse rendering for high-resolution SVBRDF estimation from an arbitrary number of images”, ACM ToG, 38(4), pp.1–15, 2019.
- [5] Z. Hui and A. Sankaranarayanan, “A dictionary-based approach for estimating shape and spatially-varying reflectance”, In Proc. ICCP2015, pp.1–9, 2015.
- [6] Z. Hui, K. Sunkavalli, J. Lee, S. Hadap, J. Wang, and A. Sankaranarayanan, “Reflectance capture using univariate sampling of BRDFs”, In Proc. IEEE ICCV2017, pp.5372–5380, 2017.
- [7] A. Ibrahim, S. Tominaga, and T. Horiuchi, “Spectral imaging method for material classification and inspection of printed circuit boards”, Optical Engineering, 49(5), 057201, 2010.
- [8] Z. Li, Z. Xu, R. Ramamoorthi, K. Sunkavalli, and M. Chandraker, “Learning to reconstruct shape and spatially-varying reflectance from a single image”, ACM ToG, 37(6), pp.1–11, 2018.
- [9] C. Liu and J. Gu, “Discriminative illumination: per-pixel classification of raw materials based on optimal projections of spectral BRDF”, IEEE Trans. PAMI, 36(1), pp.86–98, 2014.
- [10] C. Liu, G. Yang, and J. Gu, “Learning discriminative illumination and filters for raw material classification with optimal projections of bidirectional texture functions”, In Proc. IEEE CVPR2013, pp.1430–1437, 2013.
- [11] F. Pernkopf and P. O’Leary, “Image acquisition techniques for automatic visual inspection of metallic surfaces”, NDT & E International, 36, pp.609–617, 2003.
- [12] S. Tominaga and S. Okamoto, “Reflectance-based material classification for printed circuit boards”, In Proc. IEEE ICIAP2003, pp.238–244, 2003.
- [13] K. Torrance and E. Sparrow, “Theory for off-specular reflection from roughened surfaces”, JOSA, 57(9), pp. 1105–1114, 1967.
- [14] C. Wang and T. Okabe, “Joint optimization of coded illumination and grayscale conversion for one-shot raw material classification”, In Proc. BMVC2017, 2017.
- [15] L. Wolff and T. Boult, “Constraining object features using a polarization reflectance model”, IEEE Trans. PAMI, 13(7), pp.635–657, 1991.
- [16] R. Woodham, “Photometric method for determining surface orientation from multiple images”, Optical Engineering, 19(1), pp.139–144, 1980.
- [17] W. Ye, X. Li, Y. Dong, P. Peers, and X. Tong, “Single photograph surface appearance modeling with self-augmented CNNs and inexact supervision”, Computer Graphics Forum, 37(7), pp.201–211, 2018.
- [18] H. Zheng, L. Kong, and S. Nahavandi, “Automatic inspection of metallic surface defects using genetic algorithms”, Journal of Materials Processing Technology, 125–126, pp.427–433, 2002.